A Shape Memory Foam Composite with Enhanced Fluid Uptake and Bactericidal Properties as a Hemostatic Agent

T.L. Landsman[1], **T. Touchet**[1], **S.M. Hasan**[1], **C. Smith**[1], **B. Russell**[2], **J. Rivera**[2], **D.J. Maitland**[1], and **E. Cosgriff-Hernandez**[1,2,*]

[1]Department of Biomedical Engineering, Texas A&M University, College Station, Texas, 77843-3120, U.S.A

[2]Institute of Biosciences and Technology, Texas A&M University System Health Science Center, Houston, Texas 77030-3303, U.S.A

Abstract

Uncontrolled hemorrhage accounts for more than 30% of trauma deaths worldwide. Current hemostatic devices focus primarily on time to hemostasis, but prevention of bacterial infection is also critical for improving survival rates. In this study, we sought to improve on current devices used for hemorrhage control by combining the large volume-filling capabilities and rapid clotting of shape memory polymer (SMP) foams with the swelling capacity of hydrogels. In addition, a hydrogel composition was selected that readily complexes with elemental iodine to impart bactericidal properties to the device. The focus of this work was to verify that the advantages of each respective material (SMP foam and hydrogel) are retained when combined in a composite device. The iodine-doped hydrogel demonstrated an 80% reduction in bacteria viability when cultured with a high bioburden of *Staphylococcus aureus*. Hydrogel coating of the SMP foam increased fluid uptake by 19X over the uncoated SMP foam. The composite device retained the shape memory behavior of the foam with more than 15X volume expansion after being submerged in 37°C water for 15 minutes. Finally, the expansion force of the composite was tested to assess potential tissue damage within the wound during device expansion. Expansion forces did not exceed 0.6 N, making tissue damage during device expansion unlikely, even when the expanded device diameter is substantially larger than the target wound site. Overall, the enhanced fluid uptake and bactericidal properties of the shape memory foam composite indicate its strong potential as a hemostatic agent to treat non-compressible wounds.

Graphical abstract

*Corresponding author: Dr. Elizabeth Cosgriff-Hernandez, Department of Biomedical Engineering, Texas A&M University, 5033 Emerging Technologies Building, 3120 TAMU, College Station, TX 77843-3120, Tel: (979) 845-1771, Fax: (979) 845-4450, cosgriff.hernandez@tamu.edu.

Disclosures

The authors disclose that Dr. Duncan Maitland is a founder, chairman, and shareholder of Shape Memory Therapeutics, Inc. (SMT), who has an exclusive license for medical use of the shape memory polymer foam technology discussed in this research. In addition, Mr. Todd Landsman and Dr. Sayyeda Marziya Hasan are employed by SMT and hold stock options with SMT.

Shape Memory Polyurethane Foam + Antimicrobial Hydrogel Coating →
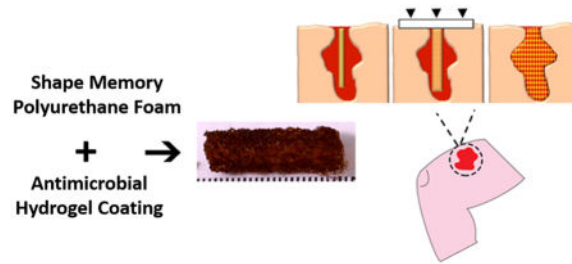
Keywords

Wound dressing; hemostasis; composite; shape memory polymer; hydrogel

1. Introduction

Hemorrhage control remains a significant concern of military and civilian trauma centers across the world. Uncontrolled hemorrhage accounts for over 30% of trauma deaths world-wide and over half of these occur before emergency care can be reached [1]. Current hemostatic treatments often rely on compression wraps or gauze as the standard of care. These treatment options are effective in ceasing the hemorrhage but are often ineffective for deep wounds that are irregularly shaped and not amenable to tourniquet application. Newer treatment options include alginates, polymer sponges, chitosan, and gauze impregnated with procoagulants, such as zeolite and kaolin [2, 3]. However, these newer technologies focus primarily on acute cessation of blood flow, rather than long-term healing and infection prevention. The three primary wound dressing technologies employed in Iraq during Operation Iraqi Freedom were HemCon® (HemCon Medical Technologies, Inc., Portland, OR), QuikClot® (Z-Medica Corporation, Wallingford, CT), and CELOX™ (SAM Medical, Tualatin, OR) [4].

HemCon® is a chitosan-based wafer which adheres to tissues upon contact with blood to effectively seal the wound boundary. This dressing has proven to be successful in establishing hemostasis in specific wounds, but the stiffness of the bandage makes packing small, narrow wounds very difficult [5, 6]. CELOX™ is another chitosan-based hemostat in which granules are poured or injected into the wound which gel together upon contact with blood to provide a physical seal that promotes hemostasis. Although CELOX™ is often deployed in civilian and military trauma situations, re-bleeding and mortality rates of 25% and 13%, respectively, have been reported [7]. QuikClot® Combat Gauze is a device consisting of gauze impregnated with kaolin, an inorganic material that has demonstrated the ability to enhance blood coagulation without causing thermal injury to wound tissue [8]. However, re-bleeding rates as high as 37% have been reported for deep, narrow wounds treated with QuikClot® Combat Gauze [9]. Although each device has proven highly effective in preventing exsanguination in the battlefield, they have proven less useful for smaller, deep wounds incurred by small-caliber firearms and improvised explosive devices [4]. Current dressings are also only indicated for a number of hours, and as such, require frequent changes to prevent bacterial and fungal infection. To address the risk of infection,

the standard of care has become the use of a broad spectrum antibiotic regimen; however, bacterial and fungal resistance has forced a series of alternative antibiotics [10].

New hemostatic technologies, such as XStat™ (RevMedx, Inc., Wilsonville, OR) have demonstrated significantly improved time to hemostasis, ease of application, and survival rates compared to conventional hemostats [11]. The XStat™ device is an applicator filled with numerous compressed cellulose sponges that rapidly expand to fill and apply pressure to deep, non-compressible wounds. Despite the numerous advantages of the XStat™ technology, the nature of inserting approximately 92 miniature sponges into an open wound can lead to a 22-fold increase in device removal time compared to conventional gauze due to the need to remove each individual sponge from the wound bed [12]. This may cause patient discomfort during prolonged device removal, as well as increased procedural time and costs.

Shape memory polymer (SMP) foams have previously demonstrated exceptional biocompatibility and hemostatic properties in porcine aneurysms [13, 14]. In acute porcine studies, SMP foams have demonstrated hemostasis within an artery in less than 90 seconds after device deployment, as determined by cessation of contrast flow past the device under x-ray [15]. The rapid hemostasis provided by the large surface area and porous morphology of the foams make them strong candidates for controlling hemorrhage. Furthermore, the ability of SMP foams to recover over >400% plastic strain during expansion would enable insertion of a small, crimped device into the wound that would rapidly expand upon contact with blood until the device is completely apposed to an irregular-shaped wound boundary, Figure 1 [16]. However, SMP foams have an inherently limited capacity for absorbing fluid [17]. In the realm of hemostatic wound dressings, the ability to absorb blood and wound fluid is critical for rapid hemostasis, wound healing, and preventing bacterial infection [18].

In this study, an antimicrobial hydrogel coating was applied to the SMP foam to create a foam-hydrogel composite with enhanced fluid uptake. Specifically, the SMP foam was coated with an n-vinylpyrrolidone (NVP) and polyethylene glycol diacrylate (PEGDA) hydrogel. In addition to increasing the fluid uptake of the composite, the hydrogel is able to directly complex with iodine to form a povidone-iodine (PVP-I_2) complex, which is one of the most widely used iodine antiseptics in surgical care. PVP-I_2 is a stable complex of polyvinylpyrrolidone (PVP) and elemental iodine that is used to kill a variety of viruses, bacteria, fungi, protozoa, and yeast, and there have been no documented cases of microbial resistance to PVP-I_2 [19]. The composite presented here combines the volume filling and rapid hemostasis of SMP foams with the fluid uptake and bactericidal action of iodine-doped hydrogels to create a highly advantageous hemostatic wound dressing prototype. The primary goal of this study was to ensure that the advantageous characteristics of the hydrogel and SMP foams were successfully combined in the composite wound dressing. To accomplish this, the first goal was to optimize the formulation of each device component. Four different hydrogel formulations were investigated for maximum fluid uptake and expansion studies were conducted on three different SMP foam formulations to determine the most rapid shape recovery. The hydrogel formulation with the greatest swelling capacity was then combined with the fastest expanding foam formulation for full characterization as a shape-memory hemostatic agent.

2. Materials and methods

2.1 Materials

All chemicals were used as received and purchased from Sigma Aldrich (Milwaukee, WI) unless otherwise noted. Foams were fabricated using N,N,N′,N′-Tetrakis(2-hydroxypropyl)ethylenediamine (HPED), 2,2′,2″-nitrilotriethanol (TEA, 98%; Alfa Aesar Inc., Ward Hill, MA), 1,6-diisocyanatohexane (HDI; TCI America Inc., Portland, OR), surfactants DC 198 and DC 5943 (Air Products and Chemicals, Inc., Allentown, PA), and deionized (DI) water (>17MΩ cm purity; Millipore water purifier system; Millipore Inc., Billerica, MA). The CellTiter 96® AQ$_{ueous}$ One Solution Proliferation Assay (Promega Corp., Madison, WI) was used for antibacterial studies to obtain a quantitative value for the absorbance of bacterial units after being cultured with iodine-containing hydrogel films.

2.2 Hydrogel Preparation

Polyethylene glycol diacrylate (PEGDA) was synthesized according to a method adapted from Hahn, et al. Briefly, 4 molar equivalents of acryloyl chloride were added dropwise to a solution of PEG (6 kDa and 10 kDa; 1 molar equivalent) and triethylamine (2 molar equivalents) in anhydrous dichloromethane (DCM) under nitrogen. After the addition was complete, the reaction was stirred for 24 hours. The resulting solution was washed with 2M potassium bicarbonate (8 molar equivalents). The product was precipitated in cold diethyl ether, filtered, and dried under vacuum. FTIR spectroscopy and proton nuclear magnetic resonance (1H-NMR) spectroscopy were used to confirm functionalization of PEGDA. Control and functionalized polymers were solution cast directly onto KBr pellets to acquire transmission FTIR spectra using a Bruker ALPHA spectrometer. Successful acrylation was indicated by an ester peak at 1730 cm^{-1} and loss of the hydroxyl peak at 3300 cm^{-1} in the spectra. Proton NMR spectra of control and functionalized polymers were recorded on Mercury 300 MHz spectrometer using a TMS/solvent signal as an internal reference. All syntheses resulted in percent conversions of hydroxyl to acrylate endgroups of greater than 90%. 1H NMR (CDCl3): 3.6 ppm (m, -OCH2CH2-), 4.3 ppm (t, -CH2OCO-) 5.8 ppm (dd, CH=CH2), 6.1 and 6.4 ppm (dd, -CH=CH2).

PEGDA-polyvinylpyrrolidone (PEG-PVP) hydrogels were prepared by dissolving PEGDA (6 kDa or 10 kDa) and N-vinylpyrrolidone (NVP) (1:96 molar ratio) to a 5 or 10 wt% solution in deionized water with a thermal initiator (1% azobisisobutyronitrile, AIBN). Hydrogels for bactericidal studies were fabricated by pipetting the precursor solution into a mold and heating to 70°C for 30 min. Iodine doping of hydrogels was conducted by placing hydrogel specimens in distilled water with 10 wt% elemental iodine for 2 hours at 50°C. Afterwards, the doped hydrogel specimens were rinsed three times with 92% ethanol, three times with distilled water, and then placed under vacuum (<0.2 mbar) to dry prior to characterization. Raman spectroscopy was utilized to confirm successful iodine complexation with the PVP. Raman spectra were recorded using a Thermo Scientific DXR Raman Microscope with a 780 nm excitation laser (max power 24 mW, 830 lines/mm gratings). Control hydrogels (PEG-I$_2$, PEG-PVP, PEG-PVP-I$_2$ no heat) were also fabricated for comparison.

2.3 Hydrogel Bactericidal Characterization

For bactericidal studies, *Staphylococcus aureus* USA 300 was cultured in tryptic soy broth overnight at 37°C while shaking at 220 RPM. Cells were diluted 1:100 in fresh tryptic soy broth and cultured for 2 hours. Cut hydrogels (PEG-PVP, PEG-PVP-I_2, 4 mm diameter) (n = 3) were placed in the bottom of 96 well plates. Gels were washed with 100 μL sterile water, 100 μL 70% ethanol, and 200 μL sterile water. 1×10^7 cells were added to each well in 100 μL media. Cells and gels were incubated for 1 hr at 37°C. After incubation, cell media was removed and the gels were washed with 100 μL sterile water. Next, 100 μL fresh tryptic soy broth was added to each well and viability assessed with the MTT assay. 20 μL/well CellTiter 96 Aqueous One tetrazolium reagent was added to each well and incubated for 4 hrs at 37°C. Absorbance was read at 490 nm per the manufacturer's instructions. In addition, bacterial suspensions from each well were diluted, plated, and counted for colony forming units after 18 hr incubation on tryptic soy broth agar plates.

2.4 SMP Foam Synthesis and Processing

Polyurethane SMP foams were fabricated using a three-step gas blowing process that has been described previously [20]. In short, an isocyanate premix of HDI was made with 39% hydroxyl groups consisting of HPED and TEA and allowed to cure for 2 days at 50°C. Then a second hydroxyl premix was made with the remaining molecular equivalents of HPED and TEA, along with surfactants (DC 198 and DC 5943) and catalysts (T-131 and BL-22; Air Products and Chemicals, Inc., Allentown, PA) in the amounts shown in Table 1. DI water was also added to the hydroxyl premix to serve as a chemical blowing agentFinally, the premixes were combined and mixed with a physical blowing agent, Enovate. The resulting foam was cured for 20 minutes at 90°C, followed by a cold cure cycle of 24 hours at room temperature, after which the foam was processed to create interconnected pores and remove any residual unreacted species within the polymer.

The first processing step the foams undergo after curing is mechanical reticulation, a process described previously by which the residual thin membranes separating the pores of the foam are removed [15]. This results in interconnected pores and the ability for fluid to penetrate the entire volume of the foam. After reticulation, the foams were cut into cylinders 10mm in diameter and 2cm in length using a 10mm biopsy punch and resistively-heated hot wire cutter. After reticulation and cutting to the desired geometry, the foam samples were extensively cleaned in a series of solutions while under sonication. This procedure included two 15 minute cycles in isopropyl alcohol (99.9% purity), four 15 minute cycles in Contrad 70® (Decon Labs, Inc., King of Prussia, PA), and two 15 minute cycles in reverse osmosis (RO) purified water. After all steps were completed, the foams were frozen in a –4°C freezer for 12 hours and subsequently freeze-dried to remove all moisture from the samples.

2.5 Composite Fabrication and Characterization

SMP foams were placed in molds (10 mm diameter x 25 mm length) and PEG-PVP precursor solutions were pipetted into the molds. A poragen mixture of dextran and saccharin was added to the hydrogel precursor solution (200 mg/mL) prior to addition to introduce pores into the hydrogel coating (particle size ~ 40–200 microns). Hydrogel-foam composites were cured at 70°C for 6 hours and the poragen leached out over the course of 2

days in deionized water. The hydrogel-foam composites were then frozen at -20°C and lyophilized. Iodine doping of composites was conducted by placing hydrogel-foam composites in distilled water with 10 wt% elemental iodine for 6 hours at 70°C. Subsequently the iodine-doped composites were frozen at −20°C in the mold and then lyophilized. Water uptake was measured in each hydrogel formulation (n = 3), the foam composition with the lowest crosslink density (H40) (n = 3), and composite specimens (n = 5) that were first dried under vacuum for 48 hours at 60°C and weighed to assess dry (polymer) mass (W_d). Each sample was then swollen in RO water for 24 hours and weighed to determine the equilibrium swelling mass (W_s). The equilibrium mass swelling ratio, Q, was calculated using the following equation:

$$Q = \frac{W_s}{W_d} \quad (1)$$

Excess fluid was removed from the exterior of each sample by resting each sample on a clean Kimwipe (Kimberly-Clark Worldwide, Inc., Roswell, GA) prior to weighing the specimen.

To determine the foam composition with the most rapid shape recovery, expansion studies were conducted on each formulation (n = 5 for each composition). To conduct these studies, the average foam diameters were measured before and after crimping using ImageJ software. Samples were then submerged in 37°C water and imaged at 30 second intervals for a total of 15 minutes. Shape recovery was calculated according to the following equation used by Dr. Tao Xie:

$$Shape\ Recovery\% = 1 - \frac{D_n - D_E}{D_c - D_E} \quad (2)$$

where D_n is the diameter of the foam at a given time point during expansion, D_E is the diameter of the expanded device before crimping, and D_c is the crimped diameter of the device [21]. To measure the average diameter of each sample, the 2-D projected surface area of the foam at each time point was divided by the length of the sample. Images were captured at each time point using a Canon PowerShot SX230 HS (Canon USA, Inc., Melville, NY) digital camera. As a scouting study to identify the effect of hydrogel formulation on shape recovery behavior, expansion studies were then repeated on composite samples that utilized each hydrogel formulation (n = 1 for each composition). Additional expansion studies were then conducted on the composition with the fastest shape recovery to determine if the expansion rate could be hastened by the incorporation of poragens into the composite device (n = 3). Finally, the volume expansion of the composite formulation with expedited shape recovery rates (n = 5) was analyzed using equation 3 below:

$$Volume\ Expansion = \left(\frac{D_n}{D_c}\right)^2 \quad (3)$$

Scanning electron microscopy (SEM) was used to assess the morphology of the wound dressing before and after hydrogel incorporation into the composite. To perform this analysis, three samples of uncoated SMP foams and iodine-doped composites were gold sputter-coated and placed on double-sided carbon tape for imaging in a NeoScope JCM5000 (Jeol USA, Inc., Peabody, MA) scanning electron microscope. Three different regions from each specimen were imaged to identify representative foam morphology.

The expansion force of composite devices was analyzed before and after the hydrogel coating was applied by following a method based on ISO 25539-2 (n = 2). For this test, devices were radially crimped to approximately 1.5mm in diameter and placed between two compression platens within a waterproof environmental chamber attached to an Instron Model 5966 Dual Column Test System (Illinois Tool Works Inc., Norwood, MA). A preload of approximately 0.15N was applied to the crimped devices before the test was initiated. After preloading, 50°C water was added to the environmental chamber to initiate device expansion until the compression platens were completely submerged. The distance between the compression platens remained constant throughout the test, while the force exerted by the expanding device was continuously measured for 15 minutes. The buoyancy force exerted by the water on the compression platens was also measured using the same method with no device between the platens. The expansion forces reported for each device are the result of subtracting the buoyancy force from the raw force measurements.

2.6 Statistical Analysis

A one-tailed, paired Student's t-Test was used with a significance level of 95% ($p < 0.05$) to determine statistical significance for fluid uptake studies. When determining the hydrogel formulation with the highest degree of swelling, as well as comparing the swelling ratio of control foams to the final composite device, a p-value of less than 0.05 was deemed a statistically significant difference. This same analysis was used for determining whether incorporation of the iodine into the hydrogels resulted in a significant reduction in bacteria viability. All data are presented as the average value for a given test with error bars equal to one standard deviation.

3. Results

3.1 Hydrogel and Foam Composition Selection

When investigating the swelling capacity of the various hydrogel formulations, the samples using 10 kDa molecular weight PEG with 5 wt% NVP demonstrated a significantly higher swelling ratio compared to the other hydrogel formulations, as shown in Figure 2A. Thus, the superior fluid uptake capacity of the PEG 10 kDa 5wt% hydrogels was selected for subsequent investigation within the final composite device. Each foam formulation (H40-H60) was also analyzed for the rate of shape recovery to determine which foam would expand most rapidly to fill a wound void and promote hemostasis. Shape recovery analysis of the three foam formulations are shown in Figure 2B. This investigation demonstrated that the foam formulation with the lowest crosslink density, H40, required the least amount of time to undergo 100% shape recovery (~ 4 minutes). Due to the rate of shape recovery, H40 foams were chosen for incorporation into the final composite device.

3.2 Iodine Doping

Raman spectroscopy peaks indicated the presence of the antibacterial polyvinylpyrrolidone-iodine ($PVP-I_2$) complex in the PEG based hydrogels, Figure 3. At lower wavenumbers, the generation of the $PVP-I_2$ complex is visible at 112 cm^{-1}. For $PEG-PVP-I_2$ complexation without heating, the peak at 112 cm^{-1} is indicative of the v_1 vibrations of I_3- complexed to PVP [22]. Upon exposure to heat, peak intensity increases and additional bands appeared around 145 cm^{-1} and 167 cm^{-1} that correspond to v_2 vibrations of I_3- and I_5-, respectively [22]. No iodine bands were visible for $PEG-I_2$ which suggests the importance of the PVP to generate an antibacterial iodophor. Additionally, no bands were visible for the PEG:PVP copolymer at lower wavenumbers since C-C peaks of this polymer are generally identified using Fourier transform infrared spectroscopy at 400 cm^{-1} and higher.

3.3 Bactericidal Properties

Iodine-doped hydrogel specimens were cultured with *Staphylococcus aureus* USA 300, a methicillin resistant strain, to determine the potential bactericidal properties of the composite. Log-phase bacterial suspensions ($\sim 1 \times 10^7$) were incubated with hydrogel specimens for 1 hr followed by quantification of bacterial viability and dilution plating of the bacterial suspension. An approximate 80% reduction in bacteria viability was observed after exposure to the iodine-doped hydrogel as compared to the positive control and the hydrogel without iodine doping, Figure 4. Results of dilution plating corroborated the viability assay (data not shown). The starting culture contained $\sim 1 \times 10^7$ staphylococci, which is equivalent to more than 1×10^8 bacteria per gram of tissue if we consider the hydrogel surface analogous to tissue. Previous studies have shown bacteria levels exceeding 1×10^5 colony forming units per gram of tissue dramatically increase the risk of infection and skin graft failure.[23, 24] Hence, the concentration of staphylococci used in these studies is representative of the bioburden typically found in wounds prone to infection and provides a rigorous test for efficacy. The rapid reduction of viable bacteria within an hour of exposure to the iodine-doped hydrogel indicates the potential bactericidal activity of the composites.

3.4 Composite Fluid Uptake

The swelling ratios of the composites were analyzed to investigate the ability to absorb wound exudate that may lead to bacterial infection and prevent healing [18]. It was also hypothesized that a higher absorptive capacity of the wound dressing will concentrate clotting factors within the dressing and enhance the rate of hemostasis [5]. Figure 5 shows SEM images of the morphology of the wound dressing before and after the hydrogel coating is applied, which shows the extent to which the hydrogel coats the struts and membranes of the foam pores to allow for enhanced fluid absorption. With the incorporation of hydrogels into the wound dressing device, there was a 19X improvement in the swelling ratio of the hydrogel-foam composite as compared to the uncoated SMP foam, Figure 6. This increase in swelling ratio directly relates to potential wound fluid uptake of the device that is critical for its function as a hemostatic agent.

3.5 Shape Recovery and Expansion Ratio

In order to ensure the composites retained the shape memory behavior of the SMP foams, expansion studies were conducted in 37°C water. First, each hydrogel composition was used to fabricate a single composite device for expansion studies to determine the effect of hydrogel formulation on expansion rate of the composite device. The results of this investigation are shown in Table 2, where the composites containing PEG 10 kDa demonstrated substantially less shape recovery after 6 minutes of submersion in a 37°C water bath than the PEG 6 kDa samples. As the priority in designing a hemostatic wound dressing is to fill large volumes and achieve hemostasis as rapidly as possible, the PEG 6 kDa composites were chosen for incorporation into the final composites due to the improved shape recovery rate. Although the use of PEG 6 kDa hydrogels resulted in a small decrease in the swelling capacity of the composite, shape recovery rate was prioritized in the design of the final device.

The final composite formulation containing PEG 6 kDa 5wt% hydrogels were then analyzed for shape recovery percentage and volume expansion after submersion in 37°C RO water. The results from this analysis are shown in Figure 7B. A typical crimped and expanded composite is shown in Figure 7A. The device would be delivered to the wound in the crimped state and would change shape to the expanded geometry upon contact with physiologic fluid at 37°C. This is possible because of the plasticization of the SMP foam upon contact with moisture, which reduces the transition temperature of the foam to approximately 10°C such that the shape memory effect will occur within the body. Expansion studies demonstrated that the composite devices retain the shape memory behavior of the SMP foams. After 15 minutes of exposure to 37°C water, the composites experienced an average shape recovery of approximately 74%. Within this time frame the device diameter more than triples, resulting in more than a 1200% increase in device volume. The volume expansion of this device over short periods of time would allow for easy delivery into narrow, penetrating wounds, and subsequent expansion to completely fill abnormal wound boundaries with a single device.

3.6 Expansion Force

An important feature of devices used to treat penetrating wounds that are not amenable to tourniquet application is the ability to apply sufficient radial force to prevent exsanguination around the device and dislocation from the wound bed under physiologic blood flow and pressure. However, the device also should not impart excessive force that may cause damage to the surrounding tissue. The forces exerted by the composites during expansion in 50°C water are summarized in Figure 8. Force measurements demonstrated an approximate 20% increase in expansion force in the composites compared to uncoated foams. The average maximum expansion force for the composite device was 0.58 N. Assuming a uniform cylindrical surface area of the crimped device, this force equates to a pressure of approximately 6.12 kPa, which is roughly equivalent to the pressure exerted by gauze within a gelatin wound model. [12]

3.7 Discussion

The ideal hemostat is capable of providing hemostasis after trauma to large vessels, requires no special preparation, is simple to apply, lightweight and durable, stable in extreme environments, causes no injury to surrounding tissues, and is inexpensive [25]. None of the dressings currently used in the field satisfy all of these criteria. The FDA approval of the XStat® (RevMedX, Wilsonville, OR) device in 2015 represents a critical advancement in addressing hemorrhage control with expandable devices. However, this device does not address potential infection issues and is only indicated for implantation for up to four hours. After this time, each of the individual sponges implanted into the body must be manually removed from the wound. The studies presented here provide proof-of-concept of the proposed shape-memory foam composite as a wound dressing with enhanced fluid uptake, antibacterial properties, and minimal risk of causing damage to the surrounding wound tissue.

Multiple hydrogel formulations were investigated for their suitability in producing an optimized wound dressing with enhanced fluid uptake and bactericidal properties. The incorporation of hydrogels into the wound dressing enabled the composite device to absorb substantially more fluid than standard surgical gauze and more fluid than many of the new hemostatic wound dressings under investigation.[12, 25] The incorporation of hydrogels increased the fluid uptake of the device 1900% compared to a device consisting entirely of SMP foam. In future iterations, the swelling capacity of the composite could be improved further through incorporation of a higher percentage of hydrogel into the composite or investigating alternative superabsorbent hydrogel formulations [26, 27]. It is also possible that reduced weight percentages of PEGDA in the hydrogel precursor solution would further improve the swelling capacity of the wound dressing.

Although current wound dressings incorporate chitosan for its hemostatic and antimicrobial effects, it is only effective against certain bacterial species and in specific pH environments. [26, 27] During this work, Raman spectroscopy revealed successful complexation of iodine into the composite to form the common surgical scrub PVP-I_2, typically sold under the brand name Betadine® (Purdue Products L.P., Stamford, CT). There have been no reported instances of microbial resistance to PVP-I_2, and as such, it makes an excellent broad spectrum antiseptic that has proven to be less of an irritant than pure iodine [19]. In antimicrobial studies investigating the effectiveness of the PVP-I_2 complexed hydrogel, there was approximately an 80% reduction in the viability of *Staphylococcus aureus* in direct contact with the hydrogel compared to the hydrogel containing no iodophors. The antibacterial results demonstrated by this hydrogel system are equivalent to the results seen in other studies investigating the antibacterial properties of silver-containing hydrogels used in medical applications [28, 29]. A limitation of this study was that the bactericidal activity of the composite device was not assessed. It is likely that the kill zone would be smaller than that seen in this study due to the porous geometry of the device and specific regions of the device that would not be in contact with the bacteria *in vitro*. However, in vivo this would likely be overcome by the diffusion of unbound iodine from the device into the surrounding area within the wound.

Expansion studies revealed that the composite device retained the shape memory behavior of the SMP foams. This allows the device to be delivered to a wound site in a small, crimped geometry and undergo more than 15X volume expansion to fill large volumes, which is more than five times greater volume expansion than new hemostatic wound dressings on the market [11]. The composites showed an average shape recovery of 74% after 15 minutes of immersion in 37°C water, which is slower shape recovery than previously demonstrated in the same composition of uncoated SMP foams [30]. When dry, the hydrogel acts as an additional moisture diffusion barrier that is likely the reason for delayed plasticization of the SMP foam and subsequent slower shape recovery. The large standard deviation during expansion studies is primarily attributable to the effects of the randomness in hydrogel orientation throughout the composite device. Agglomeration of the hydrogel in some samples at the periphery of the composite will slow the plasticization of the SMP foam and delay shape recovery compared to other samples. In order to increase the effectiveness of this device as a potential hemostat, future iterations of this device will investigate means of enhancing the rate of composite expansion. One method to accomplish this would be to reduce the amount of hydrogel used in the composite. However, this would coincidentally reduce the swelling capacity of the device. Another method to enhance the rate of expansion without affecting the swelling capacity of the device would be to isolate the hydrogel within the central core of the device so as to not cause any diffusive resistance at the periphery of the device.

Analysis of the force exerted by the composite wound dressing demonstrated an average expansion force of 0.58 N, which is approximately 20% greater than the average expansion force of uncoated SMP foams. One of the limitations of the parallel plate analysis conducted is that it only evaluates the force at the points of the device in contact with the parallel plates and ignores the total radial force exerted by the device. According to previous studies, parallel plate evaluations of the radial force of stents are approximately 10–14% of the total radial force [31]. With this understanding, the total radial expansion force of the composite may be up to 6 N- less than 20% of the radial force exerted by common vascular stents [31]. This is also assuming the wound being treated has the same diameter as the crimped device, which would likely not be the case. Given the generally accepted safety of stents and lack of adverse events related to vessel perforation, it is highly unlikely that the hydrogel-coated SMP foam composite would cause significant damage to the wound bed during expansion.

4. Conclusions

In this feasibility study, we successfully created a hydrogel-coated SMP foam that retains the advantages of each respective material system to form a composite device for the treatment of traumatic hemorrhage. This technology is capable of absorbing more fluid than many new hemostatic wound dressings currently under investigation, can undergo up to 15X volume expansion upon contact with 37°C fluid to fill large volumes, and demonstrates antibacterial properties *in vitro*. This work resulted in an initial proof-of-concept device that has shown highly valuable attributes for use as a hemostatic sponge. The composite studied here could lead to a vastly improved technology for treating hemorrhage in the battlefield and civilian trauma arena. Future studies using relevant animal models of hemorrhage will be used to further assess the potential of this device.

Acknowledgments

References

1. Kauvar DS, Lefering R, Wade CE. Impact of hemorrhage on trauma outcome: an overview of epidemiology, clinical presentations, and therapeutic considerations. J Trauma. 2006; 60:S3–11. [PubMed: 16763478]

2. Ong SY, Wu J, Moochhala SM, Tan MH, Lu J. Development of a chitosan-based wound dressing with improved hemostatic and antimicrobial properties. Biomaterials. 2008; 29:4323–32. [PubMed: 18708251]

3. Kheirabadi B. Evaluation of topical hemostatic agents for combat wound treatment. US Army Med Dep J. 2011:25–37. [PubMed: 21607904]

4. Devlin JJ, Kircher S, Kozen BG, Littlejohn LF, Johnson AS. Comparison of ChitoFlex(R), CELOX, and QuikClot(R) in control of hemorrhage. J Emerg Med. 2011; 41:237–45. [PubMed: 19345045]

5. Kozen BG, Kircher SJ, Henao J, Godinez FS, Johnson AS. An alternative hemostatic dressing: comparison of CELOX, HemCon, and QuikClot. Acad Emerg Med. 2008; 15:74–81. [PubMed: 18211317]

6. Wedmore I, McManus JG, Pusateri AE, Holcomb JB. A special report on the chitosan-based hemostatic dressing: experience in current combat operations. J Trauma. 2006; 60:655–8. [PubMed: 16531872]

7. Littlejohn LF, Devlin JJ, Kircher SS, Lueken R, Melia MR, Johnson AS. Comparison of Celox-A, ChitoFlex, WoundStat, and combat gauze hemostatic agents versus standard gauze dressing in control of hemorrhage in a swine model of penetrating trauma. Acad Emerg Med. 2011; 18:340–50. [PubMed: 21496135]

8. Johnson D, Agee S, Reed A, Gegel B, Burgert J, Gasko J, Loughren M. The effects of QuikClot Combat Gauze on hemorrhage control in the presence of hemodilution. US Army Med Dep J. 2012:36–9.

9. Sairaku A, Nakano Y, Oda N, Makita Y, Kajihara K, Tokuyama T, Kihara Y. Rapid hemostasis at the femoral venous access site using a novel hemostatic pad containing kaolin after atrial fibrillation ablation. Journal of Interventional Cardiac Electrophysiology. 2011; 31:157–64. [PubMed: 21336615]

10. Murray CK, Hsu JR, Solomkin JS, Keeling JJ, Andersen RC, Ficke JR, Calhoun JH. Prevention and management of infections associated with combat-related extremity injuries. J Trauma. 2008; 64:S239–51. [PubMed: 18316968]

11. Mueller GR, Pineda TJ, Xie HX, Teach JS, Barofsky AD, Schmid JR, Gregory KW. A novel sponge-based wound stasis dressing to treat lethal noncompressible hemorrhage. J Trauma Acute Care Surg. 2012; 73:S134–9. [PubMed: 22847084]

12. Kragh JF Jr, Aden JK, Steinbaugh J, Bullard M, Dubick MA. Gauze vs XSTAT in wound packing for hemorrhage control. Am J Emerg Med. 2015; 33:974–6. [PubMed: 25934248]

13. Rodriguez JN, Yu YJ, Miller MW, Wilson TS, Hartman J, Clubb FJ, Gentry B, Maitland DJ. Opacification of shape memory polymer foam designed for treatment of intracranial aneurysms. Ann Biomed Eng. 2012; 40:883–97. [PubMed: 22101759]

14. Rodriguez JN, Clubb FJ, Wilson TS, Miller MW, Fossum TW, Hartman J, Tuzun E, Singhal P, Maitland DJ. In vivo response to an implanted shape memory polyurethane foam in a porcine aneurysm model. J Biomed Mater Res A. 2014; 102:1231–42. [PubMed: 23650278]

15. Rodriguez JN, Miller MW, Boyle A, Horn J, Yang CK, Wilson TS, Ortega JM, Small W, Nash L, Skoog H, Maitland DJ. Reticulation of low density shape memory polymer foam with an in vivo demonstration of vascular occlusion. J Mech Behav Biomed Mater. 2014; 40:102–14. [PubMed: 25222869]

16. Sokolowski W, Metcalfe A, Hayashi S, Yahia L, Raymond J. Medical applications of shape memory polymers. Biomed Mater. 2007; 2:S23–S7. [PubMed: 18458416]

17. Yu YJ, Hearon K, Wilson TS, Maitland DJ. The effect of moisture absorption on the physical properties of polyurethane shape memory polymer foams. Smart Mater Struct. 2011:20.

18. Cutting KF. Managing wound exudate using a super-absorbent polymer dressing: a 53-patient clinical evaluation. J Wound Care. 2009; 18:200, 2–5. [PubMed: 19440172]

19. Kear TM. Does the Direct Application of Povidone-Iodine Hasten Hemostasis of the Cannulation Site After The Removal of Hemodialysis Needles? Nephrology Nursing Journal. 2012; 39:409–12. [PubMed: 23094343]

20. Singhal P, Rodriguez JN, Small W, Eagleston S, Van de Water J, Maitland DJ, Wilson TS. Ultra Low Density and Highly Crosslinked Biocompatible Shape Memory Polyurethane Foams. J Polym Sci B Polym Phys. 2012; 50:724–37. [PubMed: 22570509]

21. Xie T. Recent advances in polymer shape memory. Polymer. 2011; 52:4985–5000.

22. de Faria DLA, Gil HAC, de Queiroz AAA. The interaction between polyvinylpyrrolidone and I-2 as probed by Raman spectroscopy. Journal of Molecular Structure. 1999; 478:93–8.

23. Robson MC, Duke WF, Krizek TJ. Rapid bacterial screening in the treatment of civilian wounds. J Surg Res. 1973; 14:426–30. [PubMed: 4574478]

24. Gilliland EL, Nathwani N, Dore CJ, Lewis JD. Bacterial colonisation of leg ulcers and its effect on the success rate of skin grafting. Ann R Coll Surg Engl. 1988; 70:105–8. [PubMed: 3044237]

25. Burnett LR, Richter JG, Rahmany MB, Soler R, Steen JA, Orlando G, Abouswareb T, Van Dyke ME. Novel keratin (KeraStat) and polyurethane (Nanosan(R)-Sorb) biomaterials are hemostatic in a porcine lethal extremity hemorrhage model. J Biomater Appl. 2014; 28:869–79. [PubMed: 23594681]

26. Chung YC, Su YP, Chen CC, Jia G, Wang HL, Wu JCG, Lin JG. Relationship between antibacterial activity of chitosan and surface characteristics of cell wall. Acta Pharmacologica Sinica. 2004; 25:932–6. [PubMed: 15210068]

27. No HK, Park NY, Lee SH, Meyers SP. Antibacterial activity of chitosans and chitosan oligomers with different molecular weights. Int J Food Microbiol. 2002; 74:65–72. [PubMed: 11929171]

28. Ahearn DG, Grace DT, Jennings MJ, Borazjani RN, Boles KJ, Rose LJ, Simmons RB, Ahanotu EN. Effects of hydrogel/silver coatings on in vitro adhesion to catheters of bacteria associated with urinary tract infections. Curr Microbiol. 2000; 41:120–5. [PubMed: 10856378]

29. Yu HJ, Xu XY, Chen XS, Lu TC, Zhang PB, Jing XB. Preparation and antibacterial effects of PVA-PVP hydrogels containing silver nanoparticles. Journal of Applied Polymer Science. 2007; 103:125–33.

30. Singhal P, Boyle A, Brooks ML, Infanger S, Letts SD, Small WD, Maitland DJ, Wilson TS. Controlling the Actuation Rate of Low-Density Shape-Memory Polymer Foams in Water. Macromol Chem Phys. 2013; 214:1204–14. [PubMed: 25530688]

31. Kim DB, Choi H, Joo SM, Kim HK, Shin JH, Hwang MH, Choi J, Kim DG, Lee KH, Lim CH, Yoo SK, Lee HM, Sun K. A comparative reliability and performance study of different stent designs in terms of mechanical properties: foreshortening, recoil, radial force, and flexibility. Artif Organs. 2013; 37:368–79. [PubMed: 23461583]

## Statement of Significance

No hemostatic device currently used in civilian and combat trauma situations satisfies all the desired criteria for an optimal hemostatic wound dressing. The research presented here sought to improve on current devices by combining the large volume-filling capabilities and rapid clotting of shape memory polymer (SMP) foams with the swelling capacity of hydrogels. In addition, a hydrogel composition was selected that readily complexes with elemental iodine to impart bactericidal properties to the device. The focus of this work was to verify that the advantages of each respective material are retained when combined into a composite device. This research opens the door to generating novel composites with a focus on both hemostasis, as well as wound healing and microbial prevention.
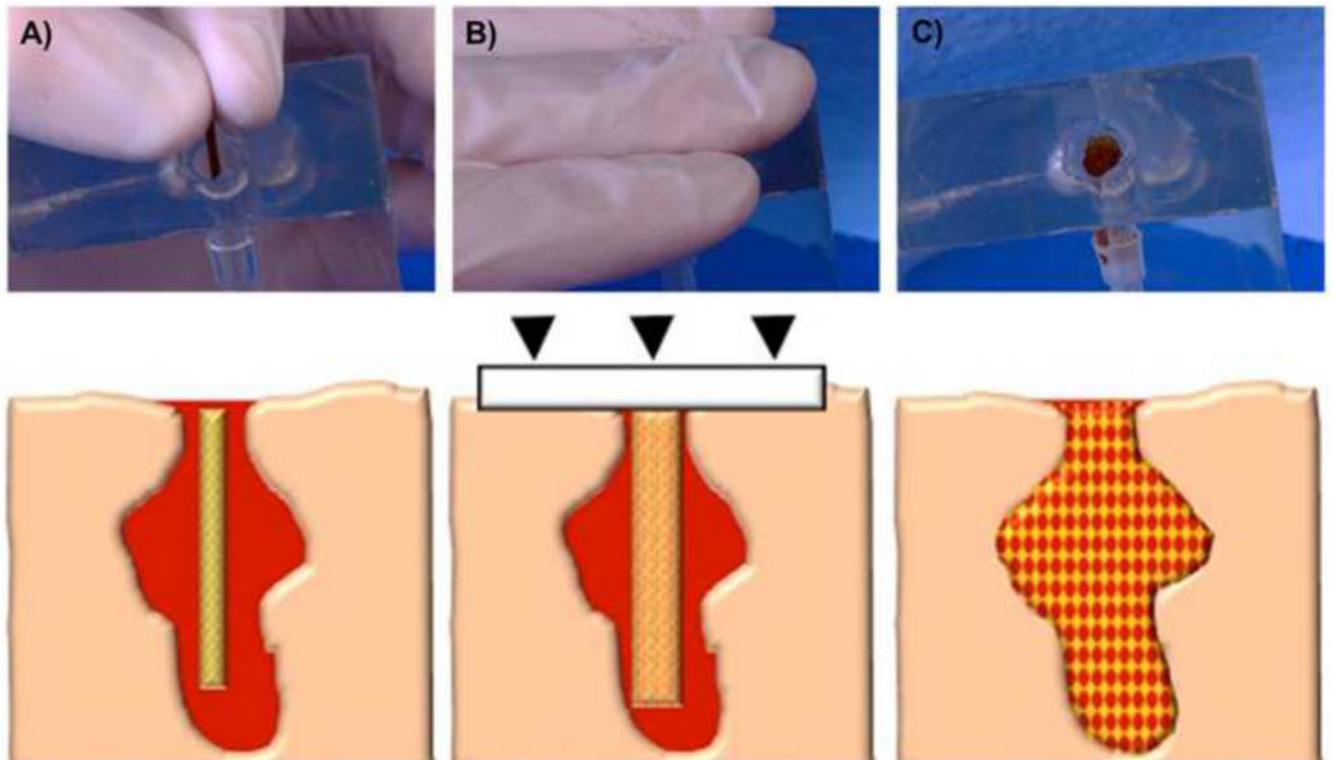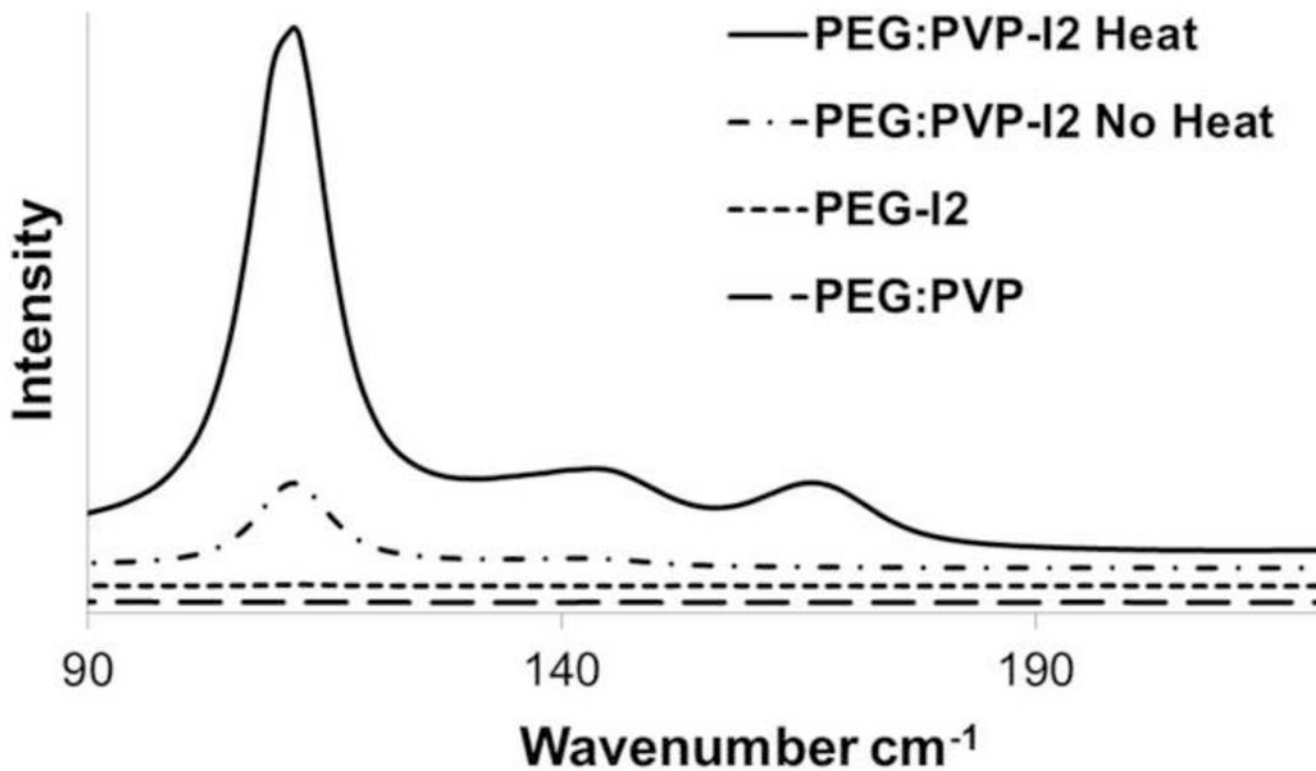
Figure 1.
Schematic of the envisioned delivery procedure for the hydrogel-SMP foam composite. The first step is to insert the crimped device into the wound (A). Then apply manual compression over the wound site to prevent the device from exiting the wound before expansion (B). Finally, the composite expands to completely fill and conform to the wound cavity and establish rapid blood clotting and hemostasis (C).
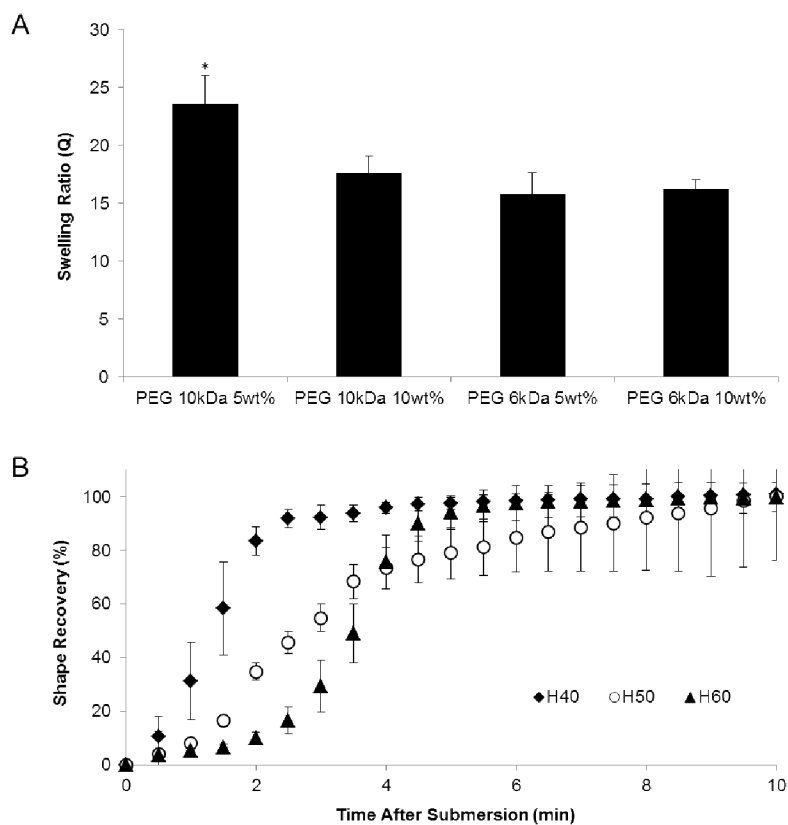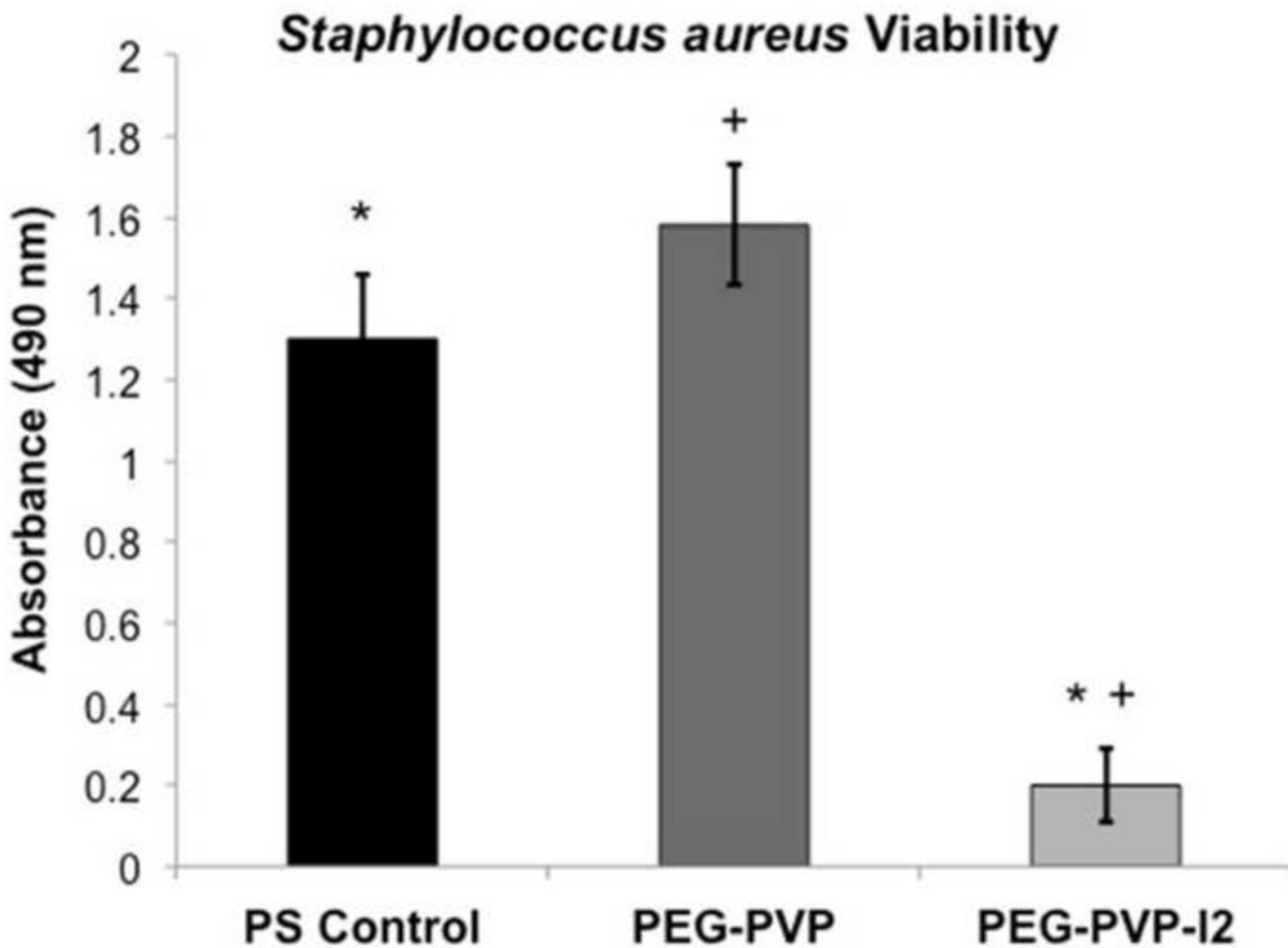
Figure 2.
A) Average swelling ratio of the hydrogel formulations investigated for potential use in the composite device. The results demonstrate a higher swelling capacity in the hydrogels utilizing 10 kDa PEG, and the highest degree of swelling with a decreased weight percentage of NVP. B) Average shape recovery percentage of the three SMP foam formulation investigated within this research when submerged in 37°C RO water, which demonstrates the most rapid shape recovery in H40 foams. The number appearing after "H" in the SMP foam nomenclature refers to the ratio of HPED to TEA equivalents within the foam composition, where the crosslink density increases as the number increases. Data shown as mean ± standard deviation (n = 3 for swelling data and n = 5 for shape recovery data). * denotes statistical significance (p = 0.05) according to one-tailed Student's t-test.

Figure 3.
Raman spectra of iodide doped hydrogels under various conditions. Successful complex of PVP and iodide is indicated by the presence of a peak at 110 cm^{-1}. A control PEG-PVP gel with no iodide is shown to confirm the lack of convolution due to the chemical composition. PEG-I$_2$ was run to confirm that the complex was due to the interactions with PVP. The heated PEG-PVP shows the greatest amount of iodide complexed to the gel.
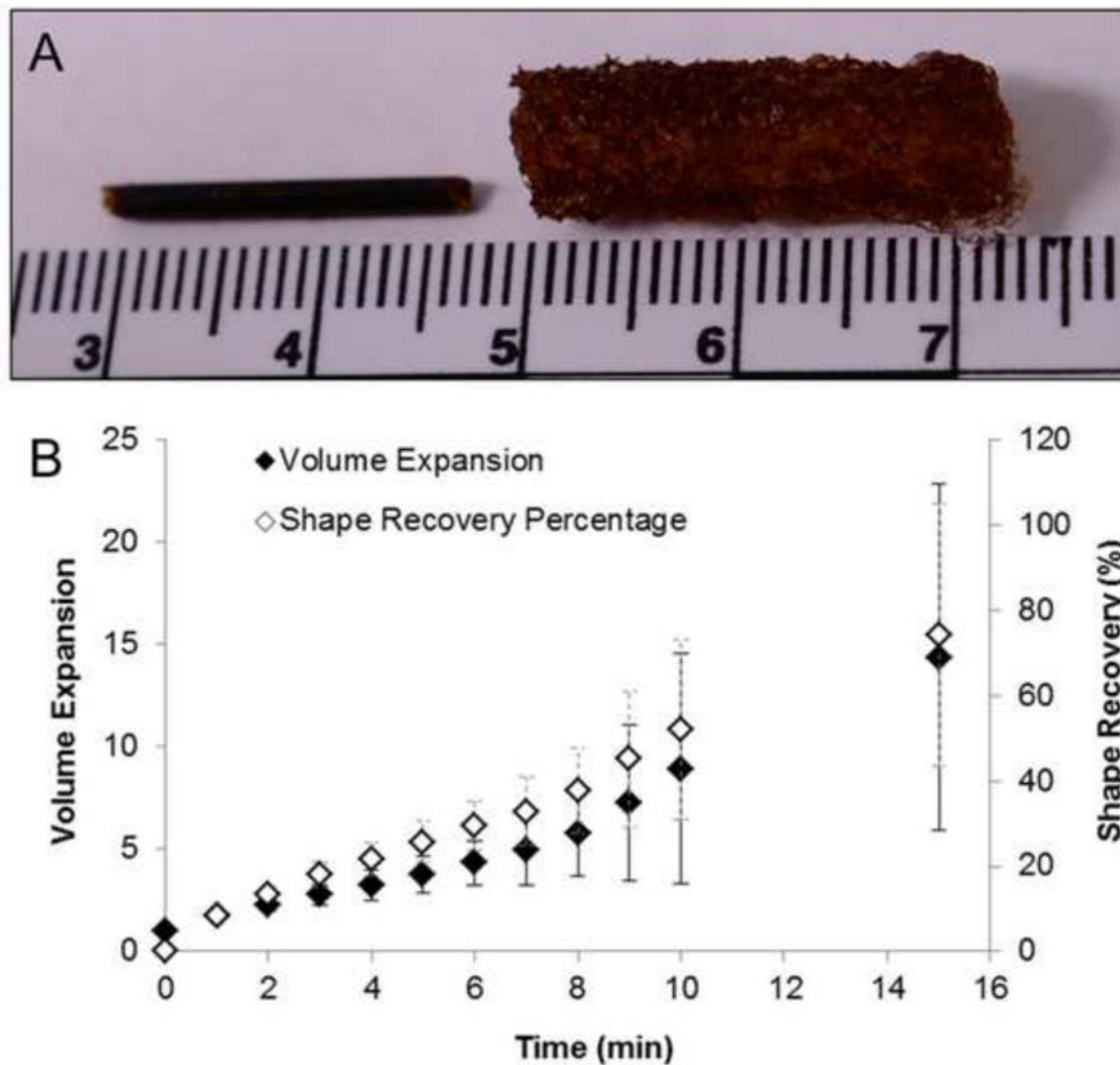
Figure 4.
Effect of the PEG-PVP hydrogel with and without iodine doping on growth of
Staphylococcus aureus measured by the MTT assay in comparison to a positive control.
Data shown as mean ± standard deviation (n = 3). * denotes statistical significance (p =
0.05) according to one-tailed Student's t-test.

Figure 5.
A) Image of uncoated SMP foam, hydrogel-foam composite, and iodine-doped composite;
B) SEM images of a SMP foam before (left) and after (right) hydrogel incorporation into the composite. After hydrogel incorporation, foam struts (solid arrow) are coated and hydrogel deposits (hollow arrow) are seen throughout the composite.
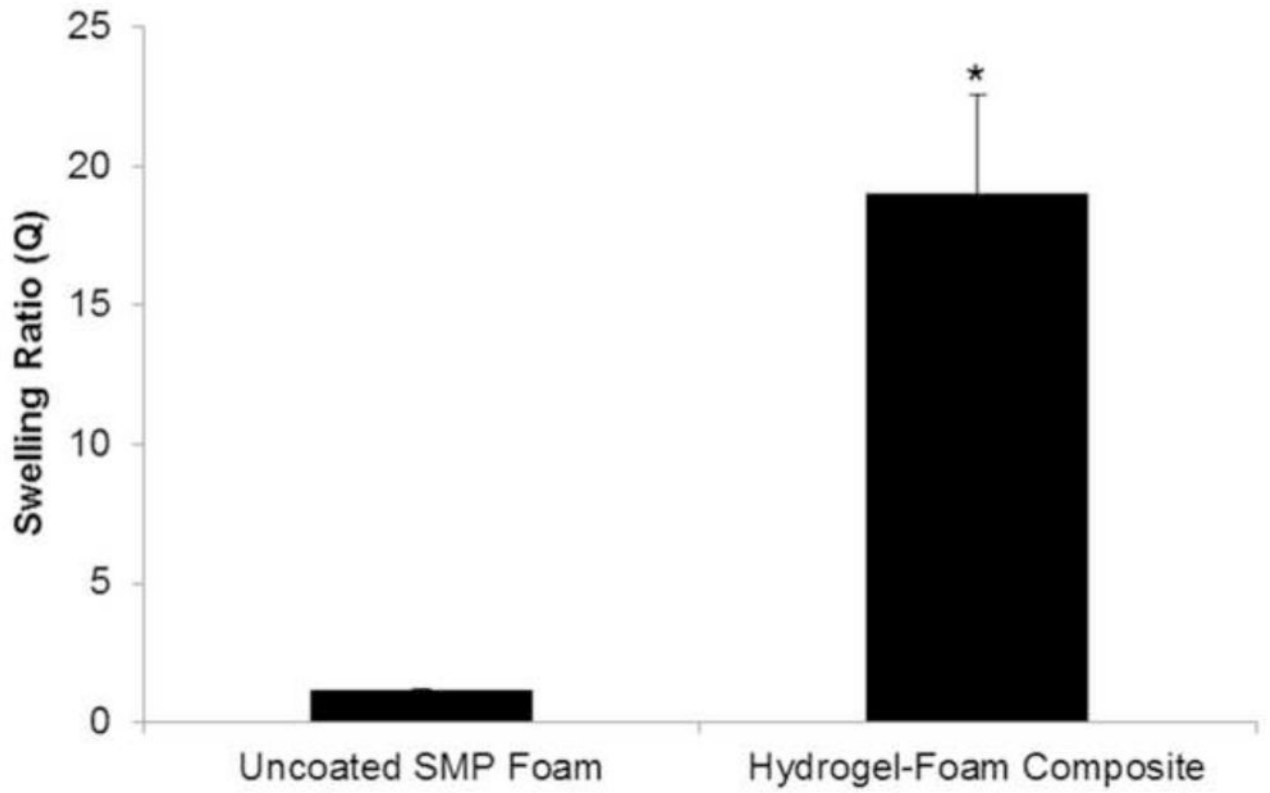
Figure 6.
Average swelling ratio of the hydrogel-foam composite consisting of PEG 6kDa hydrogel and H40 SMP foam compared to uncoated H40 SMP foams. The swelling ratio directly correlates to fluid uptake (mean ± standard deviation, n = 5). *denotes statistical significance, p = 0.05 according to one-tailed Student's t-test.
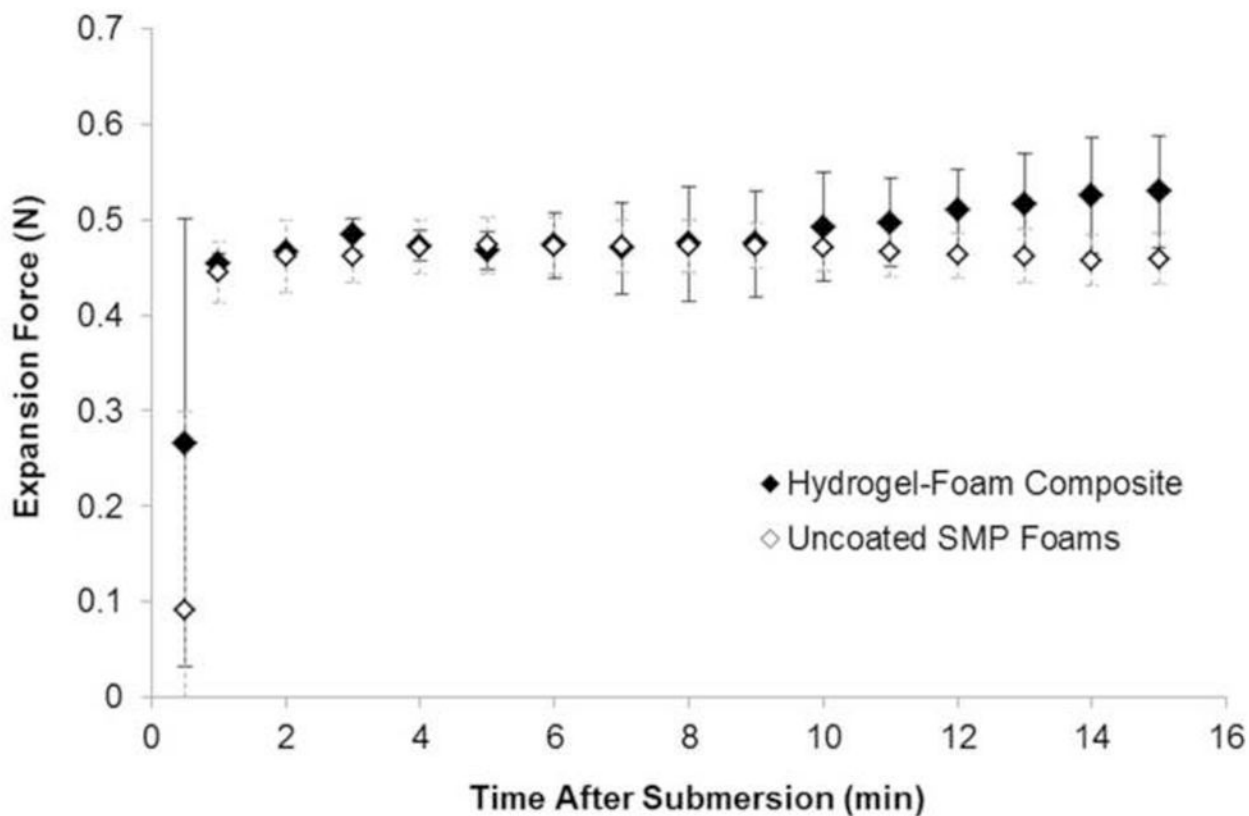
Figure 7.
A) Representative image of the appearance of a dry, crimped composite (left) and a saturated composite (right). Scale bar is in centimeters. B) Volume expansion ratio and shape recovery analysis of the wound dressing composite that incorporates the PEG 6 kDa 5wt% hydrogel and H40 SMP foam after submersion in RO water at 37°C, (mean ± standard deviation, n = 5).

Figure 8.
One dimensional force exerted by the hydrogel-foam composite and uncoated SMP foams during expansion in 50°C water (n = 2).

Table 1

Amount of constituent chemicals used in the synthesis of various SMP foam formulations.

Foam ID	HDI (wt %)	HPED (wt %)	TEA (wt %)	T-131 (wt %)	BL-22 (wt %)	DC 198 (wt %)	DC 5943 (wt %)	Water (wt %)	Enovate (PPH)
H40	63	13	13	0.3	0.6	4	3	3	4
H50	62	16	11	0.3	0.3	4	3	3	5
H60	62	19	9	0.3	0.3	4	3	3	5

Table 2

Average shape recovery percentage of composites fabricated using each of the hydrogel formulations scouted for use in the composite device (n = 1). Expansion data revealed that composites fabricated using PEG 10 kDa experienced substantially slower shape recovery than PEG 6kDa hydrogels. The selection of the PEG 6 kDa 5 wt% hydrogels for the final composite device was based on its more rapid shape recovery over the PEG 10 kDa hydrogel formulation.

Sample	Shape Recovery After 6 min (%)
PEG 6kDa 5wt%	70
PEG 6kDa 10wt%	83
PEG 10kDa 5wt%	59
PEG 10kDa 10wt%	65